Geochemical characterization of an urban lake in the centre of Rome (Lake Bullicante, Italy)

Monia Procesi (1), Daniele Cinti (1), Barbara Casentini (2), Jacopo Cabassi (3), Stefano Amalfitano (2), Luca Pizzino (1), Francesco Capecchiacci (4), Andrea Butturini (5) & Stefano Fazi (2)

ABSTRACT

Urban lakes have become increasingly important in the planning of urban ecology, green infrastructure and green areas in European cities. This paper describes the chemical, isotope and microbial features of Lake Bullicante, a small artificial lake located within the urban area of the city of Rome. It has an anthropogenic origin due to excavation works that intercepted the underlying aquifer, giving rise to a water body. The lake area is 7.000 m², with a maximum depth of 7 m and located on the distal deposits of the Alban Hills Volcanic District in an area named "Acqua Bullicante" (i.e. Bubbling Water), where degassing phenomena were historically recorded. The proximity of this volcanic district motivated the study on Lake Bullicante as a potential open-air laboratory to trace possible degassing phenomena in a highly urbanized area. A preliminary geochemical and microbial sampling survey was carried out in winter 2018. Samples were collected along a vertical profile of the lake from the surface to the maximum depth. Major, minor, trace elements, dissolved gases and stable isotopes (δD-H_2O, $\delta^{18}O$-H_2O, $\delta^{13}C$-CO_2) were analyzed, along with the analysis of $^{87}Sr/^{86}Sr$ ratio. The microbial community characteristics were analysed by epifluorescence microscopy (CARD-FISH) and flow cytometry. The chemical composition and water isotopes suggest that lake water has a meteoric origin and is related to a Ca-HCO_3 shallow aquifer hosted in volcanic rocks. This is confirmed by both the $^{87}Sr/^{86}Sr$ ratio of lake water, which falls in the range of values of Alban Hills volcanites, and the chemical-isotopic composition of neighboring wells. A relatively high concentration of dissolved CO_2, its isotopic signature ($\delta^{13}C$-CO_2 20‰ V-PDB), and the high content in organic matter (DOC 10-30 mg/L) suggest for the lake an eutrophication state with denitrification also occurring. Considering the relatively high concentrations of dissolved CO_2, an external input of carbon dioxide cannot be completely excluded and as a consequence, not even the hypothesis of mixing processes between biotic and inorganic CO_2. This makes further investigations necessary especially during the summer, when the lake is stratified. A summer survey could be also useful to better understand the microbial processes into the lake, its eutrophication evolution and health status, and to plan eventual proper remediation strategies, providing important tools to the local administration and stakeholders to improve, protect and preserve this ecological niche.

Key words: *Lake Bullicante, fluid geochemistry, microbiology, Rome, Alban Hill Volcanic District.*

(1) Istituto Nazionale di Geofisica e Vulcanologia, Via di Vigna Murata 605, 00143 Roma, Italy.
(2) Water Research Institute, National Research Council, CNR – IRSA. Via Salaria km 29.300 – CP10, 00015 Monterotondo, Roma, Italy.
(3) Institute of Geosciences and Earth Resources, National Research Council, CNR – IGG, Via La Pira 4, 50121 Firenze, Italy.
(4) Dipartimento di Scienze della Terra, Università degli Studi di Firenze, Via La Pira 4, 50121, Firenze, Italy.
(5) Department de Biologia evolutiva, Ecologia y Ciencies ambientals, Universitat de Barcelona, Catalonia, Spain.
Corresponding author e-mail: monia.procesi@ingv.it

INTRODUCTION

Urban lakes are generally man-made ecosystems resulting from excavation activities, with a surface area of a few hectares and an average depth of 3-5 m or less (Naselli-Flores, 2008). They are particularly sensitive to water pollution and eutrophication processes owing to excess enrichment of nutrients from inefficient wastewater treatment, agricultural expansion, application of chemical fertilizers and inadequate soil uses (González & Roldán, 2019; Wagner & Erickson, 2017).

Lake Bullicante (Fig. 1) is a typical example of urban lake; it is located in the eastern part of the urban area of Rome (on the left bank of Tiber River) and close to its historical centre. The lake appeared in the 1990s following illegal excavation works, which intercepted the underlying aquifer causing the rise of a small waterbody (about 7,000 m²). Due to this event and to the citizen protests, the works were suspended and the whole area expropriated. The site remained closed until 2016, favouring re-naturalization processes, new ecological systems and forbidding additional anthropogenic transformations (Battisti *et alii*, 2017).

The lake is named after the Acqua Bullicante ditch, and it is locally known also as Lake **"Ex SNIA",** from the nearby textile factory SNIA Viscosa, which was active until the early 1950. The name *Acqua Bullicante* (i.e. bubbling water) suggests the occurrence of degassing phenomena, connected to the intense and well documented hydrothermal activity which characterizes the nearest volcanic districts of the Alban Hills and the Sabatini Mountains, on whose deposits the city of Rome was built (Chiodini & Frondini, 2001; Pizzino *et alii*, 2002; Carapezza & Tarchini, 2007; Cinti *et alii*, 2017; Carapezza *et alii*, 2019; Minissale *et alii*, 2019). It is supposed that the *Acqua Bullicante* ditch was hosted along a fault (Capelli *et alii*, 2008). Camponeschi & Nolasco (1982) claimed that violent CO_2-degassing from waters was visible in the surrounding areas. However, due to the intensive uncontrolled building expansion, including the canalization and ditch covering, no trace of degassing phenomenon is visible nowadays.

In this study, we describe the geochemical features of the lake comparing chemical, isotopic and microbial characteristics, along a vertical profile from the lake surface to the bottom (~7 m). More specifically, we explored whether the target site could represent an open-air laboratory to *i*) better understand the geochemical features of the groundwater in a highly urbanized area like Rome, *ii*) trace and investigate on possible degassing

Fig. 1 - a) Panoramic view of the Lake Bullicante. b) Structure of the unlawful shopping centre. c) Researchers on INGV inflatable boat. d) Lake water sampling. (Photo credits: a) Maurizio Pastano).

phenomena and *iii*) assess main biogeochemical processes occurring. The results will contribute to proper lake environmental protection strategies, thus providing important ecosystem services to the local administrative entities and stakeholders.

GEOLOGICAL SETTING OF THE STUDY AREA

The Alban Hills Volcanic District (AHVD) is part of the Roman Comagmatic Province (Washington, 1906), a NW-striking sequence of silica-undersaturated potassic volcanic districts developed in an extensional tectonic regime along the Tyrrhenian Sea margin of central Italy. AHVD was characterised by intense volcanic activity between 600 and 20 ka and, at present, it is considered at a quiescent state (Funiciello *et alii*, 2003; Freda *et alii*, 2008; Marra *et alii*, 2003). The activity of the AHVD has been characterized by three main phases named Tuscolano-Artemisio (600-350 ka), Faete (350-270 ka) and Hydromagmatic (260-20 ka), respectively (Funiciello *et alii*, 2003; Marra *et alii*, 2003) (Fig. 2a). The volcanic products overlie sedimentary deposits constituted by sandy-silt-clay, related to the Paleo-Tiber alluvia (Pleistocene), and Pliocene marine clays.

Lake Bullicante is located in the north-eastern distal sector of the AHVD, has an elliptical shape (130 m x 80 m, in the largest point), a surface of about 7000 m^2, a maximum depth of 7 m (Fig. 2a-c) and it is hosted on the deposits of the first phase of the volcano activity, in proximity to the *Acqua Bullicante* paleo-ditch (Fig. 2d).

The whole stratigraphic sequence is displaced by a high angle NNW-SSE fault (Capelli *et alii*, 2008). The axis of the *Acqua Bullicante* ditch and the hydrographic network were probably controlled by this fault, in correspondence of which important degassing phenomena were observed (Camponeschi & Nolasco, 1982).

From a hydrogeological point of view, a shallow aquifer, hosted in the AHVD deposits, was identified in the study area and probably resulting from the merge of several aquifers that are instead well defined on the flanks of the Alban Hills (La Vigna *et alii*, 2016). This aquifer is characterized by a piezometric level between 20-25 m asl and is bounded at the base by a very low-permeability bedrock, formed by a basal clayey–sandy complex acting as aquiclude (La Vigna *et alii*, 2016).

METHODS

Field measurements

Temperature (°C), Electrical Conductivity (EC in mS/cm at 20°C), pH and dissolved O$_2$ (mg/L) were measured in winter 2018 (21st Nov) along the lake vertical profile, from the lake surface to the bottom (7 m depth) and at interval of 1 m, by using dedicated electrodes (for T, pH and EC) and gas chromatography analysis (for dissolved O$_2$). The measurements, along the entire profile, were also repeated in summer (28th June 2019) using a multi-parametric probe (Idromarambiente SCRL 1P-188A) equipped with a data logger for data storage. For details on the use of the probe and the sensors precision, refer to Cabassi *et alii* (2019). Alkalinity (Alk, mg/L) was measured in situ by acidimetric titration (AC) with 0.05 N HCl (analytical error <5%). The

water depth (m) was measured by using an echo-sounder GARMIN Stiker Plus 92 SV equipped with a transductor GT52.

Water and dissolved gases sampling and analysis

Water and dissolved gas sampling for both geochemical and microbiological analyses was carried out along lake vertical profile from the surface to the bottom at intervals of 1 m at a site corresponding to the deepest point of the lake (41°53'42" N, 12°32'20" E; 7 m depth). According to the single hose method (Tassi & Rouwet, 2014), a small diameter (6 mm) Rilsan tube, lowered at the sampling depth and connected to a 100 mL syringe equipped with a three-way Teflon valve, was used to pump up the water. After the displacement of a water volume at least twice the inner volume of the tube, one unfiltered (0.45 μm) and two filtered-acidified (with 1% HCl and ultrapure HNO$_3$, respectively) water samples were collected in polyethylene bottles for the analysis of major anions (F$^-$, Cl$^-$, SO$_4^{2-}$, NO$_3^-$ and NO$_2^-$), cations (Ca^{2+}, Mg^{2+}, NH$_4^+$, Na$^+$ and K$^+$), and trace elements (Al, V, Cr, Fe, As, Sr, Pb, Mn, B), respectively. Major elements were analysed by Ion-Chromatography (IC, Dionex ICS-900 Thermo Scientific, analytical error 5%), whereas trace elements were determined by Inductively Coupled Plasma Mass Spectrometry (ICP-MS; Agilent 7500ce, analytical error 10%). The D/^{1}H and ^{18}O/^{16}O ratios of water (expressed as δD-H$_2$O and d^{18}O-H$_2$O‰ V-SMOW) were determined on unfiltered water samples by Isotope Ratio Mass Spectrometry (IRMS). A TC-EA peripheral interfaced by means of a ConFloIV with Thermo Delta XP mass spectrometer was used for hydrogen isotopes. Oxygen isotopes measurements were carried out by using a Gas Bench peripheral coupled with a Thermo Delta V mass spectrometer. IRMS analytical error was ±0.1‰ for d^{18}O and below ±1‰ for δD. The ^{87}Sr/^{86}Sr ratio of water was determined on unfiltered water samples by a Multi-Collector ICPMS (MC-ICP-MS) coupled to a 123 nm Laser Ablation (LA) system following the procedure described by Lugli *et alii* (2017).

Water samples for the determination of dissolved gases were collected in 125 mL glass flasks equipped with a rubber septum. Dissolved gas chemistry (H$_2$, He, N$_2$, CH$_4$, CO$_2$, Ne) was determined in the free-gas phase, formed in the headspace of the sampling flasks by injecting Ar through the rubber septum, by gas chromatography (GC) using a Varian CP-4900 Micro gas chromatograph equipped with two TCD detectors and Ar as carrier gas (Capasso & Inguaggiato, 1998). The dissolved gas concentrations (expressed in bar) were calculated from the composition of the headspace gas on the basis of the solubility coefficients of each gas compound (Whitfield, 1978). Analytical error for GC was <5%. On the same sampling flasks, the ^{13}C/^{12}C isotopic ratio of Total Dissolved Inorganic Carbon (TDIC), expressed as δ^{13}C-TDIC ‰ VPDB, was analyzed by Mass Spectrometry (MS: Finnigan Delta plus XP) following the procedure described by Salata *et alii* (2000). The analytical error for MS was ±0.1‰.

Dissolved organic carbon (DOC)

The organic matter in the water was filtered onto muffled GF/F Whatman filters and collected in acid pre-
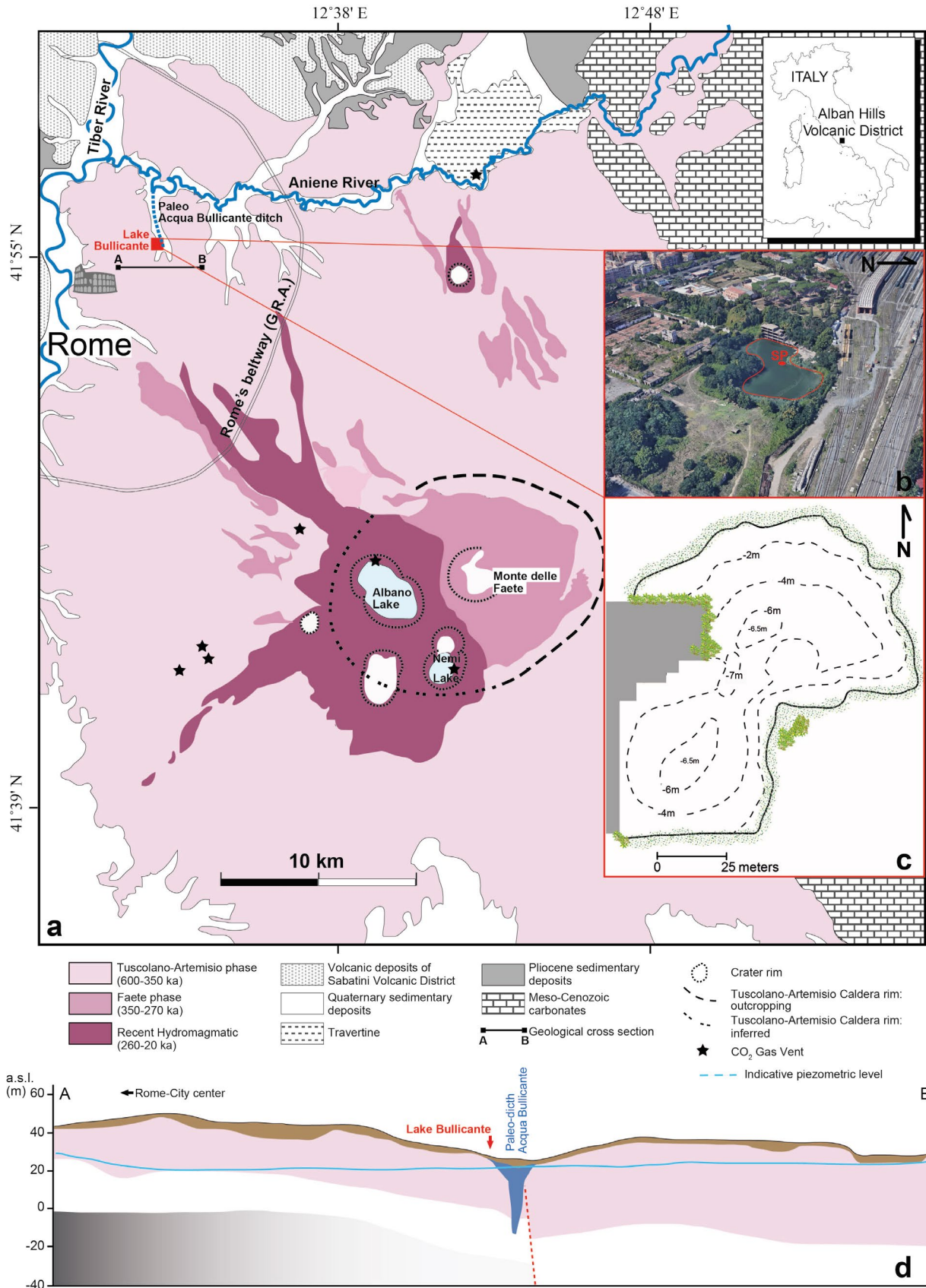
Fig. 2 - a) Simplified geological map of the AHVD (modified from MARRA *et alii*, 2009) and location of the Lake Bullicante. The three phases of volcanic activity are highlighted. b) Zoomed view on the lake, where the sampling point (SP) is also shown. c) Bathymetric map of the Lake Bullicante d) Simplified geological section (modified from CAPELLI *et alii*, 2008) passing through the study area; for the legend, see the one reported above the profile, with the exception of: brown colour for man-made fill terrains; blue for alluvia, and dashed red line for inferred fault.

washed 20 ml vials. Dissolved organic carbon (DOC) in acidified samples (HCl, Fluka Suprapur) was measured using Shimadzu TOC Analyzer.

Absorbance at 254 nm, scan in the range 270-300 nm and 350-450 nm were carried out using UV-VIS Spectrophotometer Perkin Elmer Lambda 25. These measurements were used to calculate $SUVA_{254}$ index and Spectra Slope ratio based on spectral slope $S1_{270\text{-}300}$ and $S2_{350\text{-}450}$.

Specific UV Absorbance (SUVA) is defined as the UV absorbance of a water sample at 254 nm normalized for dissolved organic carbon (DOC) concentration. Its value is strongly correlated to the aromaticity of dissolved organic matter (WEISHAAR *et alii*, 2003)

$$SUVA_{254} = \frac{Abs_{254} * ln10}{DOC * 0.01}$$

where DOC concentration is expressed in mg/L, 0.01 is the conversion factor to transform optical path from cm to m and $Abs_{254}*ln10$ corresponds to *a* the Napierian adsorption coefficient (m^{-1}).

The spectral slope (S, nm^{-1}) has been derived from DOC absorption spectra by fitting the absorption data to the equation:

$$a_\lambda = a_{\lambda_{ref}} e^{-S(\lambda - \lambda_{ref})}$$

where *a* is the Napierian absorption coefficient (m^{-1}), λ is the wavelength (nm) and λ_{ref} is the reference wavelength (nm) (TWARDOWSKI *et alii*, 2004). Two distinct spectral slope regions (275-295 nm and 350-400 nm) within log-transformed absorption spectra were used to evaluate organic matter transformation (S_1 and S_2) (HELMS *et alii*, 2008). The ratio S_R of the slope S_1 and S_2 is then calculated:

$$S_R = \frac{S1}{S2} = \frac{slope\ 275 - 295}{slope\ 350 - 400}$$

SR provides information about molecular size, origin and photodegradation. Thus, high proportion of the DOM molecular fraction with low molecular weight and photodegradation determine increase of S_R values. For the analysis of microbial community, lake waters (50 mL) were collected at 9 depths. Moreover, aliquots (250 mL) were collected at 5 depths (0, 1, 3, 5, 7 m depth), fixed on-site with formaldehyde solution (37% w/v, Sigma Aldrich; final concentration 1%), and stored at 4°C for 2 h.

MICROBIOLOGICAL SAMPLING AND ANALYSES

To assess the abundance of Bacteria and Archaea, sub-aliquots of 5–10 mL were filtered at low vacuum levels (<0.2 bar) onto 0.2 μm pore-size polycarbonate filters (type GTTP; diameter, 47 mm; Millipore, Eschborn, Germany). Filters were stored at -20°C until further processing. Filter sections were stained with DAPI at a final concentration of 1 μg/mL to quantify the total Prokaryotes. Community composition was assessed by fluorescence in situ Hybridization Catalyzed Reported Deposition (CARD-FISH) as described in TASSI *et alii* (2018). In particular, rRNA-target Horseradish peroxidase (HRP) labeled

oligonucleotidic probes (Biomers, Ulm, Germany) were used to target Bacteria (EUB338 I-III), and Archaea (ARCH915).

The abundance of total prokaryotes and pigmented phytoplanktonic microorganisms (i.e., Cyanobacteria, pico- and nano-Eukaryotes) were determined by the Flow Cytometer A50-micro (Apogee Flow System, Hertfordshire, UK), equipped with a 20 mW Solid State Blue Laser (488 nm) and a 16 mW Solid State UV laser (375 nm). The light scattering signals (forward and side light scatter named FSC and SSC, respectively), red fluorescence (>610 nm), orange fluorescence (590/35 nm), and blue fluorescence (430–470 nm) were acquired and considered for the direct identification and quantification of distinct microbial groups by following harmonized protocols (GASOL & MORÁN, 2015). Total prokaryotes were quantified by following the staining procedure with SYBR Green I (1:10000 dilution; Life Technologies, code S7563). Thresholding was set on the green channel, and gating strategy was manually adjusted to exclude most of the unspecific signals according to negative unstained controls. Cyanobacteria, pico- and nano-Eukaryotes were characterized and distinguished according to their pigmentation (i.e., reflecting on different intensities of autofluorescence signals collected at the orange and red channels) and size (i.e., proportionally related to light scatter signals). Thresholding was set on the red channel in order to exclude most of the unspecific signals according to 0.2-μm filtered control water samples. The gating strategy was manually adjusted on the density plots of SSC versus Red and of Orange versus Red channels. The volumetric absolute counting was carried out in density plots of SSC versus blue channel. Data handling and visualization were performed by the Apogee Histogram Software (v89.0).

RESULTS

WATER TEMPERATURE, EC, PH AND DISSOLVED O₂

Temperature, pH, EC and dissolved O_2 concentrations measured along the vertical profiles of Lake Bullicante are shown in Fig. 3a-d. During the winter survey, water temperature (~15°C) did not display significant variation with depth. In the summer, the lake surface was warm (up to 28°C) and a thermocline was recognized at 1-4 m depth (Fig. 3a) separating a relatively warm epilimnion (28°C) from a cold hypolimnion (11°C). The pH followed a similar vertical pattern to temperature: it was relatively constant in the winter (~7.5), whereas in the summer, it showed a *S* shape profile, with high values (between 8 and 9) up to 2 m depth, then progressively decreasing to values around 7 towards the bottom (Fig. 3b). The EC was constant (~770μS/cm) in the winter along the entire vertical profile (Fig. 3c). In June, the EC profile was marked by three chemoclines, the shallowest one in correspondence of the thermocline, the main one at 2-6 m depth and the third one at 7 m depth. Dissolved O_2 concentrations, during the winter, did not display significant variation with depth (~0.12±0.3 mg/L), whereas in the summer it had a strong decrease with depth, disappearing immediately below 2m depth (Fig. 3d).
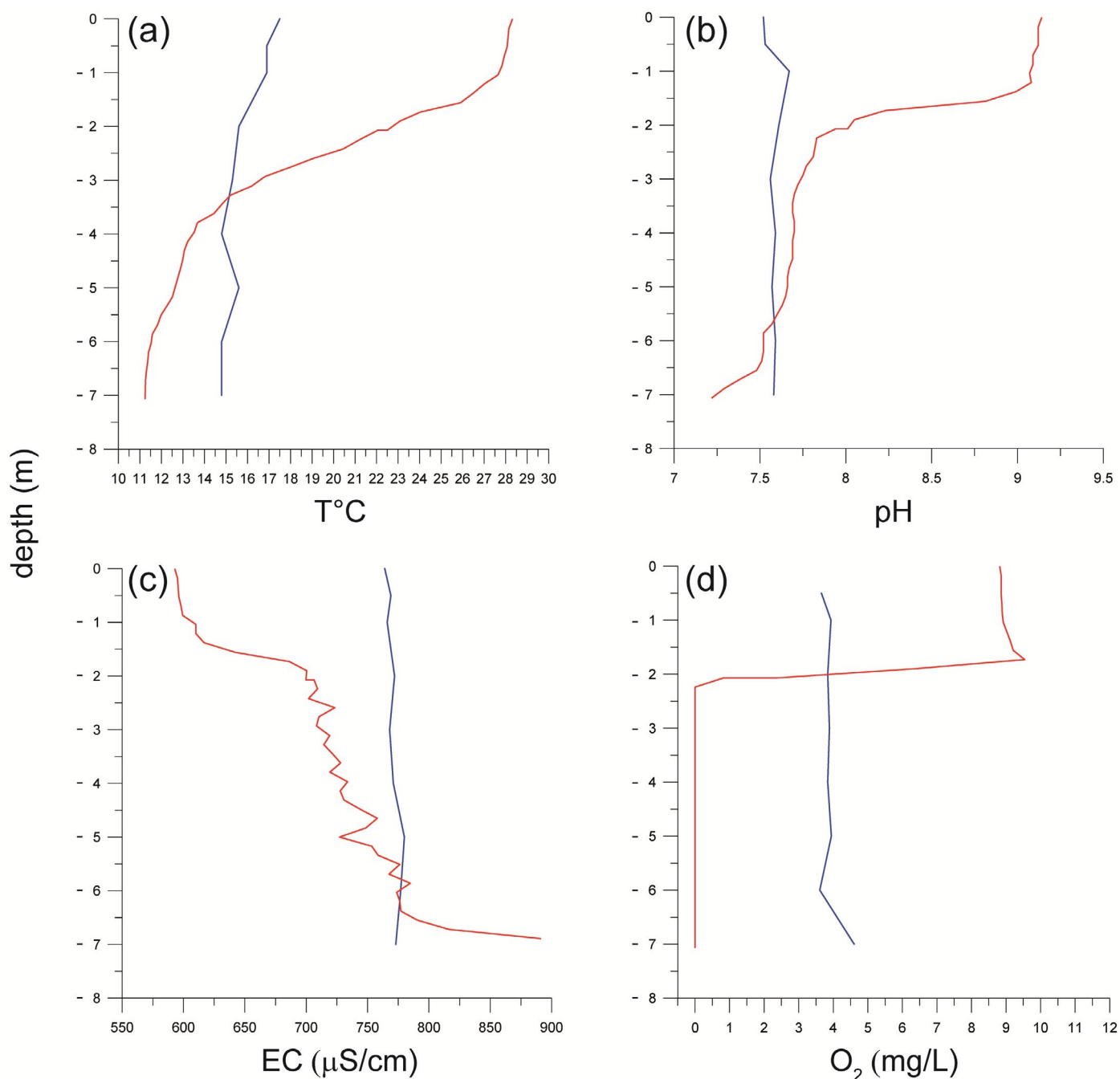
Fig. 3 - Winter (blue) and summer (red)vertical profiles along the Lake Bullicante water column of a) water temperature (°C); b) pH, c) electrical conductivity (EC, in µS/cm) and d) dissolved O_2 concentration (in mg/L).

CHEMICAL AND ISOTOPIC COMPOSITION OF LAKE WATER AND DISSOLVED GASES

The lake water was characterized by total dissolved solids (TDS) up to 704 mg/L and a Ca(Mg)-HCO_3 composition, and showed relatively constant concentrations of the two major ions (Ca^{2+} and HCO_3^- concentrations up to 72 and 415 mg/L, respectively) from the lake surface to the bottom (Fig. 4a-b, Tab. 1). Concentrations of F^-, Cl^-, SO_4^{2-}, Na^+, K^+ and Mg^{2+} were up to 2.3, 37, 46, 35, 45 and 26 mg/L, respectively and were nearly constant through the vertical lake profile (Fig.4b-d, Tab. 1). Nitrogen species showed a different behavior. As NH_4^+ concentrations were nearly

constant from the lake surface to the bottom (0.44 to 0.59 mg/L), NO_3^- ranged from 6 to 10 mg/L in the upper 4 m and decreasing to 0.26 mg/L at 5 m depth (Fig. 4d), whereas NO_2^- showed a reverse trend, being lower in the upper 4 m (up to 2.9 mg/L) and higher towards the lake bottom (up to 6.3 mg/L).

As far as minor and trace elements concentration is concerned, relatively constant concentrations of B, Sr (up to 0.12 and 1.0 µg/L, respectively) V, Cr, Fe, Mn, As and Pb (up to 22, 1.3, 5.2, 53, 12 and 0.38 µg/L, respectively) were recorded, whereas the aluminum abruptly decreased from 13 to 3.1 µg/L between 0 and 1 m depth, then irregularly ranged from 0.51 to 3.1 µg/L in the interval from 1 to 4 m
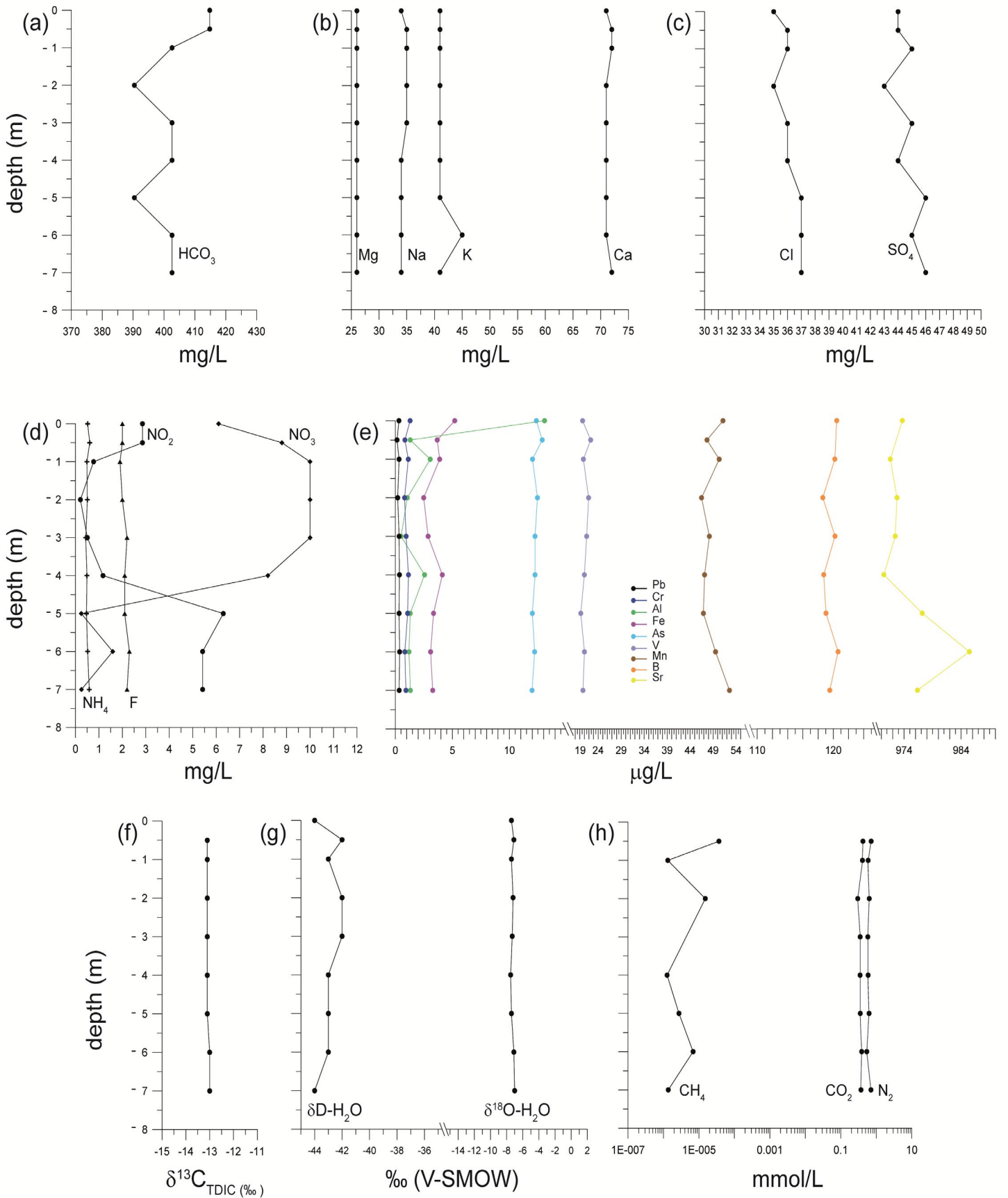
Fig. 4 - Vertical profile along the Lake Bullicante water column of a) HCO_3 concentration; b) Mg, Na, K and Ca concentrations; c) Cl and SO_4 concentrations; d) NO_3, NO_2, NH_4 and F concentrations; e) trace element (Pb, Cr, Al, Fe, As, V, Mn, B and Sr) concentrations; f) $\delta\,^{13}C\text{-}CO_2$ value (‰ vs. V-PDB), g) $\delta D\text{-}H_2O$ and $\delta^{18}O\text{-}H_2O$ values and h) dissolved CH_4, CO_2 and N_2 concentrations.

TABLE 1

Chemical composition of the water sampled from the Lake Bullicante. Sampling depth (in m), temperature (T, in °C), pH, Total Dissolved Solids (TDS, in mg/L) and concentrations of the main ions (HCO_3^-, F^-, Cl^-, NO_2^-, NO_3^-, SO_4^{2-}, Ca^{2+}, Mg^{2+}, Na^+, K^+, NH_4^+, PO_4^{3-} in mg/L) and traces elements (Al, V, Cr, Fe, As, Sr, Cd, Pb, Mn and B, in µg/L) are reported. The $\delta^{18}O$-H_2O (‰ vs. V-SMOW), δD-H_2O (‰ vs. V-SMOW), and $\delta^{13}C$-TDIC (in ‰ vs. V-PDB) and $^{87}Sr/^{86}Sr$ values are also reported; nd: not determined.

Depth	T	pH	TDS	HCO_3^-	F^-	Cl^-	NO_2^-	NO_3^-	SO_4^{2-}	Ca^{2+}	Mg^{2+}	Na^+	K^+	NH_4^+	PO_4^{3-}
0	17.8	7.5	704	415	2.0	35	2.9	6.1	44	71	26	34	41	0.52	<0.10
1	16.9	7.7	697	403	1.9	36	0.77	10	45	72	26	35	41	0.49	<0.10
2	15.6	7.6	681	390	2.0	35	0.21	10	43	71	26	35	41	0.51	<0.10
3	15.3	7.6	696	403	2.2	36	0.51	10	45	71	26	35	41	0.44	<0.10
4	14.8	7.6	693	403	2.1	36	1.2	8.2	44	71	26	34	41	0.49	<0.10
5	15.6	7.6	681	390	2.1	37	6.3	0.25	46	71	26	34	41	0.47	<0.10
6	14.8	7.6	697	403	2.3	37	5.4	1.6	45	71	26	34	45	0.52	<0.10
7	14.8	7.6	693	403	2.2	37	5.4	0.26	46	72	26	34	41	0.59	<0.10

Depth	Al	V	Cr	Fe	As	Sr	Pb	Mn	B	$\delta^{13}C_{TDIC}$	$\delta^{18}O$-H_2O	$\delta^{18}D$-H_2O	$^{87}Sr/^{86}Sr$
0	13	21	1.3	5.2	12	974	0.32	51	120	-13.1	-7.4	-44	nd
1	3.1	21	1.1	3.9	12	972	0.33	50	120	-13.1	-7.1	-42	0.710403
2	1.1	22	0.81	2.5	12	973	0.21	46	119	-13.1	-7.4	-43	nd
3	0.51	22	0.95	2.9	12	972	0.33	48	120	-13.1	-7.2	-42	nd
4	2.6	21	1.2	4.1	12	970	0.36	47	119	-13.1	-7.3	-42	nd
5	1.3	20	1.1	3.4	12	977	0.33	47	119	-13.1	-7.5	-43	nd
6	1.2	21	0.84	3.1	12	985	0.38	50	121	-13.0	-7.4	-43	nd
7	1.3	21	0.93	3.3	12	976	0.34	53	120	-13.0	-7.1	-43	nd

depth and stabilized near 1.3 µg/L towards the lake bottom (Fig. 4e).

The $\delta^{13}C$-TDIC values were constant with depth at the value of -13‰ vs. V-PDB (Fig. 4f). The $\delta^{18}O$-H_2O and δD-H_2O values varied in a narrow range from -7.0 to -7.5‰ and from -42 to -44‰ vs. V-SMOW, respectively (Fig. 4g). No clear trends with depth were observed by these isotopic parameters. The $^{87}Sr/^{86}Sr$ ratio was analyzed at the sampling depth of 1 m and showed a value of 0.7104.

The chemical (mmol/L) and isotopic composition ($\delta^{13}C$-CO_2) of dissolved gases is reported in Tab. 2. Nitrogen and CO_2 were largely dominant in the lake profile (N_2 from 0.54 to 0.72 mmol/L, CO_2 from 0.35 to 0.42 mmol/L; Fig. 4h), whereas O_2 and CH_4 were relatively lower (from 0.11 to 0.14 mol/L and from 1.3×10^{-6} to 3.7×10^{-5} mmol/L, respectively). None of them showed clear trend with depth. He and H_2 were detected only at the lake bottom, with concentrations of 3.9×10^{-6} and 5.7×10^{-6} mmol/L, respectively.

The $\delta^{13}C$ values of dissolved CO_2 were calculated from the $\delta^{13}C$-TDIC values using the empirical equation of ZHANG *et alii* (1995), as follows:

$$\delta^{13}C\text{-}CO_2(g) = \delta^{13}C_{TDIC} - \frac{H_2CO_3}{TDIC}\varepsilon\,(H_2CO_3 - CO_2) - \frac{HCO_3^-}{TDIC}\varepsilon\,(HCO_3^- - CO_2) - \frac{CO_3^{2-}}{TDIC}\,(CO_3^{2-} - CO_2)$$

where the equilibrium molar ratios of aqueous carbon species at sampling temperature and pH, used in equation showed above, were computed with the PHREEQC code

(PARKHURST & APPELO, 2013), whereas the value given by DEUSER & DEGENS (1967) and MOOK *et alii* (1974) was used for the isotope fractionation factor (ε) between gaseous CO_2 and dissolved (CO_{2aq}). The $\delta^{13}C$-CO_2 values ranged from -21.2 to -21.6‰ V-PDB (Tab. 2).

TABLE 2

Main dissolved gases (N_2, O_2, CH_4, CO_2, He, H_2, in mmol/L) from Lake Bullicante. Sampling depth (m) and isotopic composition of dissolved CO_2 ($\delta^{13}C$-CO_2 in ‰ vs. V-PDB) are also reported; bdl: below detection limit.

Depth	N_2	O_2	CH_4	CO_2	He	H_2	$\delta^{13}C$-CO_2
0.5	0.72	0.11	3.7E-05	0.42	bdl	bdl	-21.2
1	0.63	0.12	1.5E-05	0.41	bdl	bdl	-21.3
2	0.58	0.12	bdl	0.35	bdl	bdl	-21.6
3	0.59	0.12	1.3E-06	0.35	bdl	bdl	-21.6
4	0.63	012	2.7E-06	0.35	bdl	bdl	-21.6
5	0.54	0.12	6.9E-06	0.35	bdl	bdl	-21.5
6	0.71	0.11	1.4E-06	0.39	bdl	bdl	-21.5
7	0.63	0.14	1.5E-05	0.37	3.9E-06	5.7E-06	-21.5

ORGANIC MATTER

Mean dissolved organic carbon (DOC) content in Lake Bullicante was 15.3±9.6 mg/L with a decreasing trend with depth (Tab. 3) and a maxima at 0.5 m and a minima at the bottom (Fig.5a). Spectral slope ratio (S_R) profile resembled DOC trend. All values, except 1.68 at 0.5 m depth, were below 1 ($S_2 > S_1$) and ranging from 0.54 to 0.9 (Fig. 5b). Calculated $SUVA_{254}$ values decreased from 0.96 to 0.72 between 1 and 5 m depth and then increased to 1.75 at the bottom of the lake (Fig. 5c).

The total microbial load in sampled waters was generally high. The prokaryotic abundance ranged between 1×10^7 and 2×10^7 cells/ml, with microscopy and flow cytometry showing consistently similar results and patterns. The occurrence of pigmented phytoplanktonic microorganisms was in the range of values reported for eutrophic lake waters (Cyanobacteria = $0.6-1.1 \times 10^5$ cells/ml; Pico-Eukaryotes = $7.6-9.5 \times 10^3$ cells/ml; Nano-Eukaryotes = $1.1-6.1 \times 10^2$ cells/ml) without any consistent differences along the water column (Fig. 5d-g). CARD-FISH analysis showed that Bacteria represented 65% -75% of total DAPI stained cells, while Archaea 6% - 8%.

DISCUSSION

Relatively low TDS (<1000 mg/L) and Ca-HCO$_3$ composition are typical features of groundwater hosted in the volcanic aquifers of the Roman Magmatic Province and Roman area (CHIODINI & FRONDINI, 2001; CINTI et alii. 2017; PIZZINO, 2015). The chemical composition of waters from wells located near Lake Bullicante (PIZZINO, 2015) (Fig. 6a-
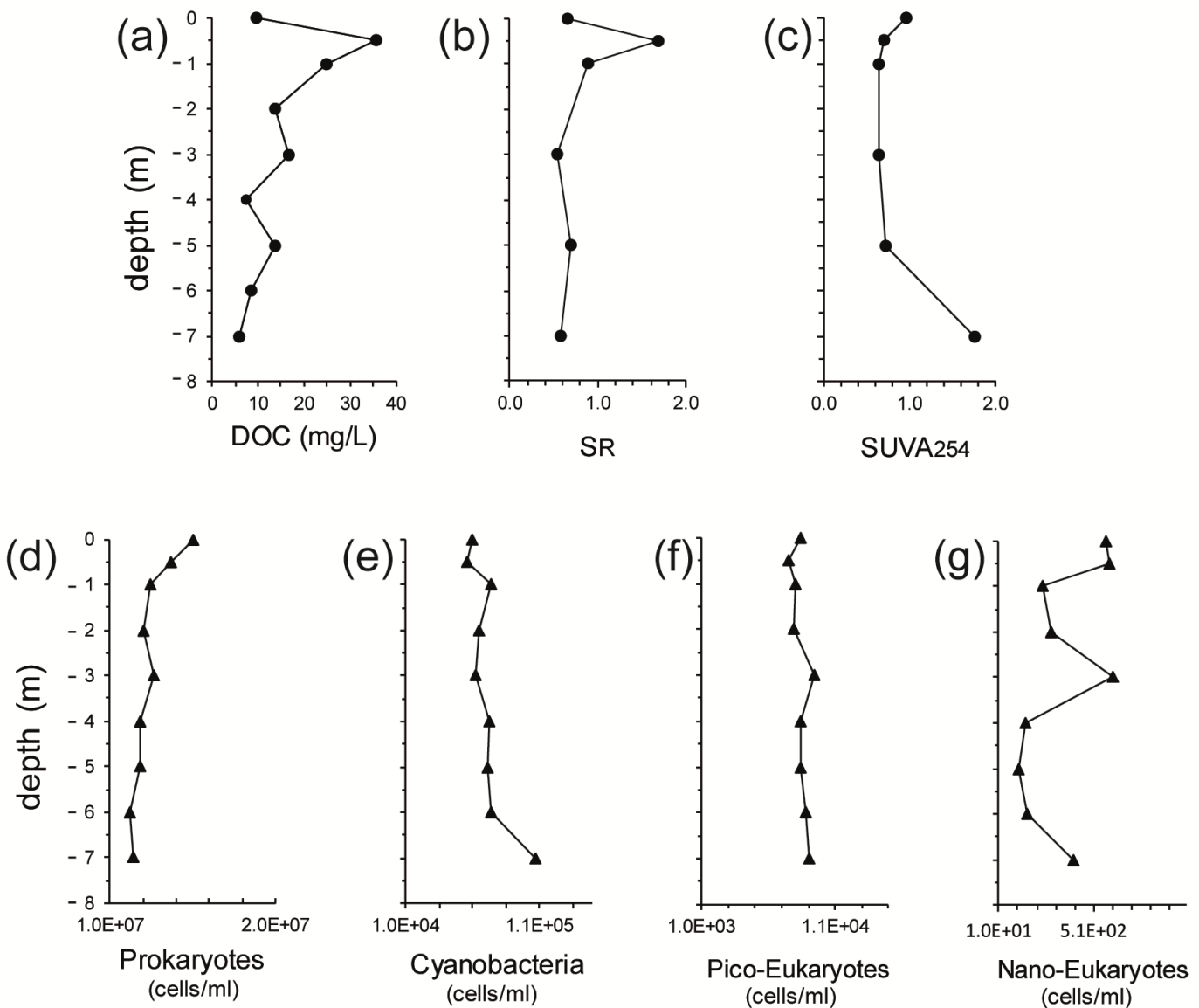

Fig. 5 - Vertical profile along the Lake Bullicante water column of a) dissolved organic carbon (DOC); b) spectra slope ratio (SR) based on spectral slope S1$_{270-300}$ and S2$_{350-450}$; c) specific UV absorbance (SUVA$_{254}$) of the water sample at 254 wavelength; d) abundance of prokaryotes.; e-g) occurrence of pigmented phytoplanktonic microorganisms (Cyanobacteria, Pico-Eukaryotes, Nano-Eukaryotes).

TABLE 3

Microbial composition in water samples from the Lake Bullicante. Sampling depth (in m), dissolved organic carbon (DOC, mg/L), spectral slope ration (S_R), absorbance at 254 nm ($SUVA_{254}$), and Prokaryotes, Cyanobacteria, pico- and nano-Eukaryotes abundances (in Cells/mL) are reported; nd: not determined.

| Depth	DOC	S_R	$SUVA_{254}$	Prokaryotes	Cyanobacteria	PicoEukaryotes	NanoEukaryotes
0	9.7	0.65	0.96	1.50E+07	5.95E+04	8.44E+03	5.77E+02
0.5	37.5	1.68	0.70	1.37E+07	5.62E+04	7.57E+03	5.98E+02
1	25	0.90	0.65	1.24E+07	7.43E+04	8.03E+03	2.40E+02
2	13.7	nd	nd	1.20E+07	6.45E+04	7.91E+03	2.83E+02
3	16.8	0.54	0.64	1.26E+07	6.30E+04	9.48E+03	6.14E+02
4	7.5	nd	nd	1.18E+07	7.23E+04	8.36E+03	1.53E+02
5	13.8	0.70	0.72	1.18E+07	7.10E+04	8.48E+03	1.11E+02
6	8.3	nd	nd	1.12E+07	7.40E+04	8.79E+03	1.63E+02
7	5.7	0.58	1.75	1.14E+07	1.07E+05	9.10E+03	4.02E+02
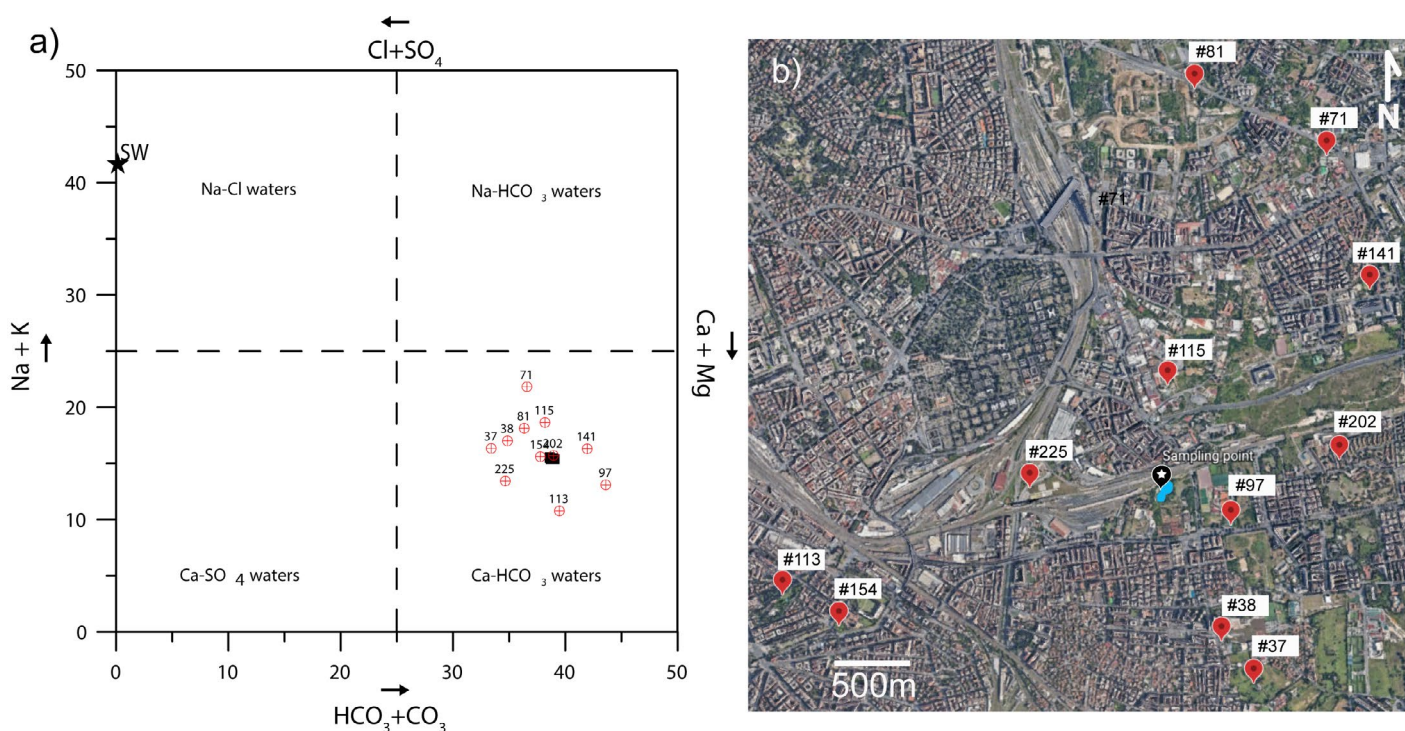
Fig. 6 - a) Langelier-Ludwig square diagram and comparison between the lake water (black squares) and the waters from wells (red circles) from PIZZINO (2015); b) location of the water wells (from #37 to #225) nearby the lake (Sampling Point).

b), which are fed by shallow, low-temperature reservoirs hosted within volcanic formations, closely resembles lake water. This suggests that the hydrological circuit feeding the lake is closely related to the volcanic aquifer feeding the wells. This is consistent with the relatively high content of F⁻ and K⁺ of the lake water since volcanic products of the Roman Magmatic Province are typically enriched in these elements (GAMBARDELLA *et alii*, 2005; DE RITA *et alii*, 2011).

As shown in the $\delta^{18}O$ vs. δD diagram (Fig. 7), where the Global Meteoric Water Line (GMWL; Craig, 1961), the Mediterranean Meteoric Water Line (MMWL; GAT & GARMI, 1970) and the waters from wells from PIZZINO (2015) are reported, the isotopic signature of lake and well waters,

is consistent with that of meteoric water, confirming that both of them are related to the same aquifer hosted in the volcanic rocks and fed by a meteoric recharge. For all groundwater, the low-temperature environment is highlighted by the absence of $\delta^{18}O$ positive shifts.

The aquifer is hosted in the distal Alban Hills volcanic products related to the first phase of volcanic activity. In this regard, the comparison among the $^{87}Sr/^{86}Sr$ isotopes ratio of the Alban Hills volcanites (in the range 0.71029-0.71057, e.g. BOARI *et alii*, 2009), the lake and the water collected from a nearby well (#202, Fig. 6b), shed light on their common origin. This relationship is well shown in Fig. 8 where $^{87}Sr/^{86}Sr$ of both rocks and groundwater
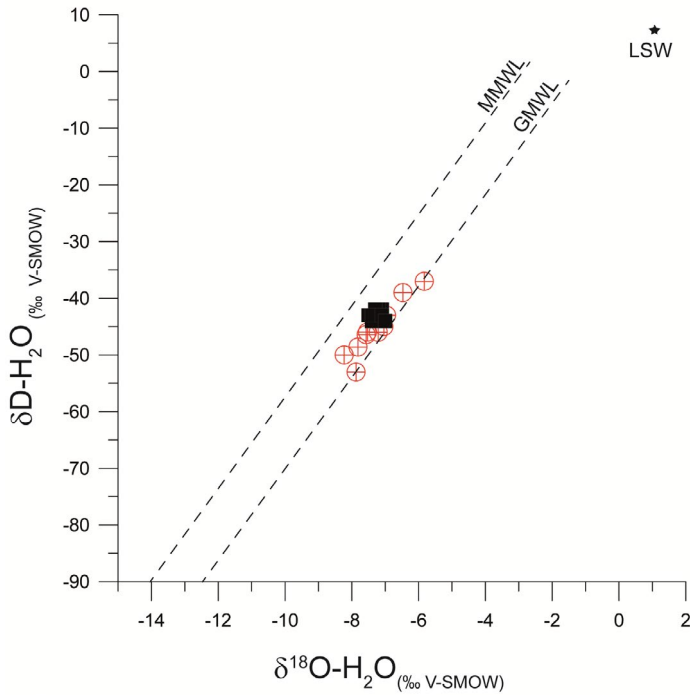
Fig. 7 - δD-H₂O vs. δ¹⁸O-H₂O diagram for Lake Bullicante and waters from neighboring wells from PIZZINO (2015). The dashed lines delineate the isotopic domain for Global Meteoric Waters (GMWL; $\delta D = 8 d^{18}O + 10$; CRAIG, 1961) and that for Mediterranean Meteoric Waters (MMWL; $\delta D = 8 d^{18}O + 22$; GAT & CARMI, 1970), respectively. LSW = local seawater. Symbols as in Fig. 6.
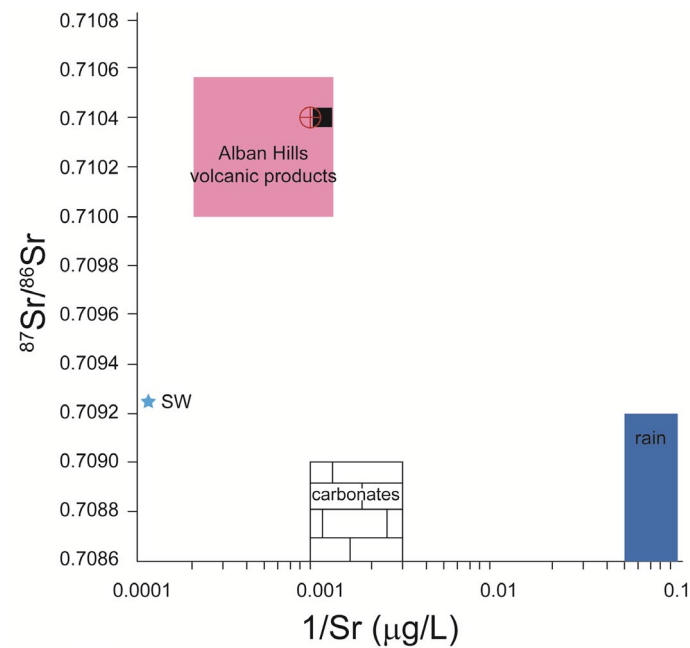
are plotted against 1/Sr. Data clearly show that both water (lake and well) have the same isotopic value and lie in the field of the Alban Hills volcanites.

Since lake water chemistry was analyzed during the winter survey, it is not surprising that it does not show significant variations along the vertical profile, both for major and trace elements. An exception is represented by the nitrate and nitrite concentrations, i.e. the significant decrease of NO_3^- at 3-5 m depth and the simultaneous increase of the NO_2^-. The excess of NO_2^- can be related to synthetic fertilizers, mineralized fertilizer and in particular to degradation of soil organic matter, denitrification processes or contamination by manure and/or sewage. In our case, the increase of NO_2^- and the simultaneous decrease of NO_3^- suggests the occurrence of degradation of organic matter and in particular, denitrification processes, where nitrate is reduced to produce molecular nitrogen (N_2) through a series of intermediate products, such as NO_2^- (CLARK & FRITZ, 1997; MAYER et alii, 2002).

As observed for lake water chemistry, the composition of dissolved gases does not show significant changes along the vertical profile. The most striking features of Lake Bullicante is the relative high concentrations of dissolved CO_2 along the whole vertical profile and as suggested by the N_2-CO_2-O_2 ternary diagram (Fig. 9), where the concentrations of dissolved gases of the lake water and the adjacent wells (PIZZINO, 2015) are reported. The relatively low and high concentration of dissolved O_2 and CO_2 respectively, along the vertical profile of the lake may be ascribed to processes that take place in the lake itself. Generally speaking, major processes controlling O_2 and CO_2 in freshwater lakes, are i) the enhanced biological productivity resulting from high input of nutrients and ii) the high organic matter supply provided by soil erosion
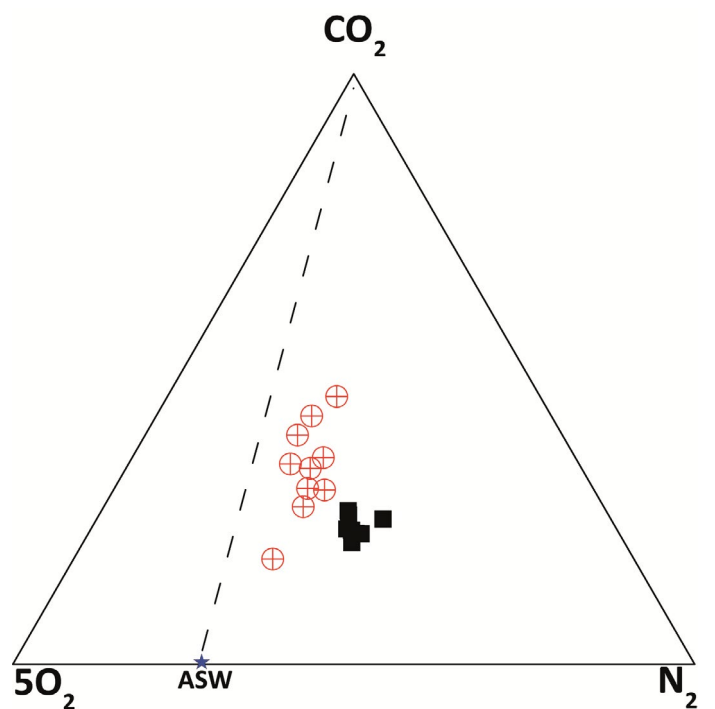

Fig. 8 - ⁸⁷Sr/⁸⁶Sr vs. 1/Sr of Lake Bullicante water sample and a water sample from a well taken as representative of the volcanic aquifer (see text). For comparison, ⁸⁷Sr/⁸⁶Sr values/ranges of Alban Hills volcanic rocks (e.g. BOARI et alii, 2009), Apennine carbonate rocks (e.g. BARBIERI et alii, 1979), seawater (sw, e.g. VEIZER, 1989) and rainwater (e.g. PEARCE et alii, 2015), are also shown. Symbols as in Fig. 6.

Fig. 9 - N₂-CO₂-O₂ ternary diagram for dissolved gases. Molar concentrations are expressed in mmol/L. ASW = air saturated water at 20°C. Symbols as in Fig. 6.

in the drainage areas (Likens, 1972). Nutrient overloading may produce the eutrophication of lakes, a condition that tends to be more frequent in urban environments than in natural systems (Schueler & Simpson, 2001; Naselli-Flores, 2008; Liang et alii, 2019).

The calculated $\delta^{13}C$ values lower than -21‰ V-PDB, suggest a biogenic source of CO_2 (Cerling et alii, 1991) and support the hypothesis of the high input of nutrients, a related enhanced biological productivity and as a consequence suggest possible eutrophication of the lake. However, considering that i) past degassing phenomena in the study area (Camponeschi & Nolasco, 1982) have demonstrated the rise of isotopically "heavier" CO_2 deriving from crustal-mantle inorganic sources (e.g., Chiodini & Frondini, 2001; Cinti et alii, 2017) and that ii) the CO_2 of the adjacent wells is likely of mixed biogenic and inorganic source (Pizzino, 2015), the hypothesis of an inflow of inorganic CO_2 into the lake cannot be completely excluded. This makes further investigations necessary especially during the summer, when the lake is stratified.

DOC concentration confirms the trophic condition generally attributed to eutrophic lakes with residence time of years. Lakes with reduced volumes are reported to have DOC above 10 mg/L and this is quite uncommon for largest lakes (Hanson et alii, 2003; Sobek et alii, 2007; Hanson et alii, 2011). DOC peak of about 40 mg/L at 0.5 just below the surface (0.5 m depth) is most probably due to the accumulation of less degradable organic matter products of photobleaching degradation, that is common in organic rich lakes (Brinkmann et alii, 2003) with intense microbial activities. This is also confirmed by the increased value of S_R at this depth. S_R increase due to photodegradation or input autochthonous humid organic matter and decrease due to microbial activity in dark layers (Helms et alii, 2008). SR decreases towards the bottom of the lake due to most probably to the release of aromatic organic matter from bottom sediments. Extremely low $SUVA_{254}$ values are likely related to photodegradation processes or the contribution of autochthonous organic matter of small dimensions. $SUVA_{254}$ is a good indicator of the humic fraction of the DOC (Weishaar et alii, 2003). In rivers, a value of 5-10 is common and an increase is generally observed due to sediment contribution. In our case, this explains the highest SUVA value at water sediment interface (Fig. 5 c).

Cell abundance values is one or two orders of magnitude higher that those found in surface waters of the central Italian lakes (Fazi et alii, 2016; Tassi et alii, 2018), underlining the eutrophication state of the Lake Bullicante. Values similar to those registered in Lake Bullicante, were found in the deepest layers of meromitic volcanic lakes, highly loaded in nutrients, in eutrophic Tyrrhenian coastal lakes and wastewaters (Pizzetti et alii, 2016; Amalfitano et alii, 2018; Tassi et alii, 2018). The occurrence of phytoplanktonic microorganisms (Cyanobacteria, Pico-Eukaryotes, Nano-Eukaryotes) was also relatively high, with no consistent changes along the depth, and with values comparable to those found in lake waters at high nutrient levels and blooming conditions (Callieri, 2008; Trombetta et alii, 2019). This could indicate a complete remixing of the water columns during winter, in comparison with the clear thermal stratification in summer, and a high rate of microbial respiration in water that counterbalance primary production, resulting in a low oxygen concentration along the entire water column.

Conclusion

This study was motivated by the possibility to use the Lake Bullicante as potential open-air laboratory to trace, in a highly urbanized area as Rome, possible degassing phenomena related to the nearby Alban Hills Volcanic District, because violent CO_2-degassing from waters were historically here recognized. Our results show that the hydrological circuit feeding the lake is closely related to the shallow volcanic aquifer feeding the nearby water wells. Moreover, the relatively high concentration of biogenic CO_2 and the high content of organic matter, highlight that the lake is eutrophic and denitrification processes also occurring. The absence of anomalous concentration in phosphates, ammonium and sulphates, proxies of contamination, strengthen the hypothesis of denitrification and exclude possible sewage input. Isotopic analyses of N_2 and O_2 of NO_3^- along the entire water column could provide more detailed information, to definitively exclude the idea of potential contamination. Nevertheless, considering the past inorganic CO_2 degassing phenomena occurred in the study area related to crustal-mantle sources, and that, both the lake and adjacent wells present relatively high concentrations of dissolved CO_2, an external-lake input of CO_2 cannot be completely excluded, and as a consequence, not even the hypothesis of mixing processes between biotic and inorganic CO_2. This makes further investigations necessary especially during the summer, when the lake is stratified and even more CO_2 could build up near the bottom of the lake. A summer survey could be also useful to better understand the microbial processes in the lake because the high abundance in organic matter, recorded along the winter profile of the lake, could have important implications for the trophic state of the lake, bringing to potential toxic blooms. The results of further campaigns would contribute to deeply understand the eutrophication evolution of the lake, its health status and plan eventual proper remediation strategies such as, in-lake actions and lake basin management, providing important tools to the local administration and stakeholders to improve, protect and preserve this important aquatic system.

REFERENCES

Amalfitano S., Levantesi C., Garrelly L., Giacosa D., Bersani F. & Rossetti S. (2018) - *Water quality and total microbial load: a double-threshold identification procedure intended for space applications.* Front. Microbiol., **9**, 2903.

BATTISTI C., DODARO G. & FANELLI G. (2017) - *Paradoxical environmental conservation: Failure of an unplanned urban development as a driver of passive ecological restoration.* Environmental Development, **24**, 179-186.

BARBIERI M., MASI U. & TOLOMEO L. (1979) - *Origin and distribution of strontium in the travertines of Latium (Central Italy).* Chem. Geol., **24**, 181-188.

BOARI E., AVANZINELLI R., MELLUSO L., GIORDANO G., MATTEI M., DE BENEDETTI ARNALDO A., MORRA V. & CONTICELLI S. (2009) - *Isotope geochemistry (Sr–Nd–Pb) and petrogenesis of leucite-bearing volcanic rocks from "Colli Albani" volcano, Roman Magmatic Province, Central Italy: inferences on volcano evolution and magma genesis.* Bull. Volcanol., **71**, 977–1005.

BRINKMANN T., SARTORIUS D. & FRIMMEL F.H. (2003) - *Photobleaching of humic rich dissolved organic matter.* Aquat. Sci., **65**, 415-424.

CABASSI J., CAPECCHIACCI F., MAGI F., VASELLI O., TASSI F., MONTALVO F., ESQUIVEL I., GRASSA F. & CAPRAI A. - *Water and dissolved gas geochemistry at Coatepeque, Ilopango and Chanmico volcanic lakes (El Salvador, Central America).* J. Volcanol. Geother. Res., **378**, 1-15.

CALLIERI C. (2008) - *Picophytoplankton in freshwater ecosystems: the importance of small-sized phototrophs.* Freshwater Reviews, **1**, 1-28.

CAMPONESCHI B. & NOLASCO F. (1982) - *Roma e i Colli Albani.* In: Le risorse naturali della regione Lazio, Vol. **7**.

CAPASSO G. & INGUAGGIATO S. (1998) - *A simple method for the determination of dissolved gases in natural waters. An application to thermal waters from Vulcano Island.* Appl. Geochem, **13**, 631-642.

CAPELLI G., MAZZA R. & TAVIANI S. (2008) - *Acque sotterranee nella città di Roma.* Mem. Descr. Carta Geol. D'It. LXXX, pp. 221-245.

CARAPEZZA M. L., BARBERI F., RANALDI M., TARCHINI L., & PAGLIUCA N.M. (2019) - *"Faulting and gas discharge in the Rome area (Central Italy) and associated hazards".* Tectonics, **38**, 941–959.

CARAPEZZA M.L. & TARCHINI L. (2007) - *Accidental gas emission from shallow pressurized aquifers at Alban Hills volcano (Rome, Italy): geochemical evidence of magmatic degassing?* J. Volcanol. Geotherm. Res., **165**, 5-16.

CERLING T.E., SOLOMON D.K., QUADE J. & BOWMAN J.R. (2019) – *On the isotopic composition of carbon in soil carbon dioxide.* Geoch. Cosmoch. Acta, **55**, 3403-3405.

CHIODINI G. & FRONDINI F. (2001) – *Carbon dioxide degassing from the Albani Hills volcanic region, Central Italy.* Chem. Geol., **177**, 67–83.

CINTI D., TASSI F., PROCESI M., VASELLI O. & VOLTATTORNI N. (2017) – *Geochemistry of hydrothermal fluids from the eastern sector of the Sabatini Volcanic District (central Italy).* App. Geoch., **84**, 187-2011.

CLARK I. & FRITZ P. (1997) – *Environmental isotopes in hydrogeology.* Lewis Publishers, Boca Raton, New York, 328pp.

CRAIG H. (1961) – *Isotopic variations in meteoric waters.* Science, **133**, 1702–1703.

DE RITA D., CREMISI C., CINNIRELLA A. & SPAZIANI F. (2011) - *Fluorine in the rocks and sediments of volcanic areas in central Italy: Total content, enrichment and leaching processes and a hypothesis on the vulnerability of the related aquifers.* Environmental Monitoring and Assessment, **184**, 5781-5796.

DEUSER W.G. & DEGENS E.T. (1967) - *Carbon isotope fractionation in the system CO_2 (gas)-CO_2 (aqueous)-HCO_3 (aqueous).* Nature, **215**, 1033-1035.

FAZI S., CROGNALE S., CASENTINI B., AMALFITANO S., LOTTI F. & ROSSETTI S. (2016) - *The arsenite oxidation potential of native microbial communities from arsenic-rich freshwaters.* Microb. Ecol., **72**, 25-35.

FREDA C., GAETA M., MISITI V., MOLLO S., DOLFI D. & SCARLATO P. (2008) - *Magma-carbonate interaction: an experimental study on ultrapotassic rocks from Alban hills (Central Italy).* Lithos, **3-4**, 397-415.

FUNICIELLO R., GIORDANO G. & DE RITA D. (2003) - *The Albano Maar lake (Colli Albani Volcano, Italy): recent volcanic activity and evidence of pre-Roman Age catastrophic lahar events.* J. Volcanol. Geotherm. Res., **123**, 43–61.

GAMBARDELLA B., MARINI L. & BANESCHI I. (2005) - *Dissolved potassium in the shallow groundwaters circulating in the volcanic rocks of central-southern Italy.* App. Geochem., **20**, 875-897.

GONZÁLEZ E. J. & ROLDÁN G. (2019) - *Eutrophication and Phytoplankton: Some Generalities from Lakes and Reservoirs of the Americas. Microalgae - From Physiology to Application.* Ed. Milada Vítová. IntechOpen. https://doi.org/10.5772/intechopen.89010

GASOL J.M. & MORÁN X.A.G. (2015) - *Flow cytometric determination of microbial abundances and its use to obtain indices of community structure and relative activity.* In: McGenity, T., Timmis, K., Nogales B. (Eds.) Hydrocarbon and Lipid Microbiology Protocols. Springer Protocols Handbooks. Springer, Berlin, Heidelberg.

GAT J.R. & CARMI I. (1970) - *Evolution of the isotopic composition of atmospheric waters in the Mediterranean Sea area.* J. Geophys. Res., **75**, 3039–3048.

HANSON P.C., BADE D.L., CARPENTER S.R. & KRATZ T.K. (2003) *Lake metabolism: Relationships with dissolved organic carbon and phosphorus.* Limnol Oceanogr., **48**, 1112-1119.

HANSON P.C., HAMILTON D.P., STANLEY E.H., PRESTON N., LANGMAN O.C. & KARA E.L. (2011) - *Fate of Allochthonous Dissolved Organic Carbon in Lakes: A Quantitative Approach.* PLoS ONE, **6**, e21884.

HELMS J.R., STUBBINS A., RITCHIE J.D., MINOR E.C., KIEBER D.J. & MOPPER K. (2008) - *Absorption spectral slopes and slope ratios as indicators of molecular weight, source, and photobleaching of chromophoric dissolved organic matter.* Limn. Oceanogr., **53**, 955-969.

LA VIGNA F., MAZZA R., AMANTI M., DI SALVO C., PETITTA M., PIZZINO L., PIETROSANTE A., MARTARELLI L., BONFÀ I., CAPELLI G., CINTI D., CIOTOLI F., CIOTOLI G., CONTE G., DEL BON A., DIMASI M., FALCETTI S., GAFÀ R.M., LACHINI A., MANCINI M., MARTELLI S., MASTRORILLO L., MONTI G.M., PROCESI M., ROMA M., SCIARRA A., SILVI A., STIGLIANO F. & SUCCHIARELLI C. (2016) - *Groundwater of Rome.* J. Maps, **12**, 88-93.

LIANG J., HUANG C., STEVENSON M.A., QIAO Q., ZENG L. & CHEN X. (2019) - *Changes in summer diatom composition and water quality in urban lakes within a metropolitan area in central China.* Int. Rew. Hydrobiol., https://doi.org/10.1002/iroh.201801953

LIKENS G.E. (1972) - *Mirror Lake – its past, present and future?* Appalachia, **39**, 23-41.

LUGLI F., CIPRIANI A., PERETTO C., MAZZUCCHELLI M. & BRUNELLI D. (2017) - *In situ high spatial resolution $^{87}Sr/^{86}Sr$ ratio determination of two Middle Pleistocene (ca 580 ka) Stephanorhinus hundsheimensis teeth by LA–MC–ICP–MS.* Int. J. Mass Spectrom., **412**, 38–48.

MARRA F., FREDA C., SCARLATO P., TADDEUCCI J., KARNER D.B., RENNE P.R., GAETA M., PALLADINO D.M., TRIGILA R. & CAVARRETTA G. (2003) - *Post-caldera activity in the Alban Hills volcanic district (Italy): 40Ar/39Ar geochronology and insights into magma evolution.* Bull. Volcanol., **65**, 227–247.

MARRA F., KARNER D.B., FREDA C., GAETA M. & RENNE P.R. (2009) - *Large mafic eruptions at Alban Hills Volcanic District (CentralItaly): Chronostratigraphy, petrography and eruptive behavior.* J. Volcanol. Geother.Res., **179**, 217-232.

MAYER B., BOYER E.W., GODALE C., JAWORSKI N.A., BREEMEN N.V., HOWARTH R.W., SEITZINGER S., BILLEN G., LAJTHA K., NADELHOFFER K., DAM D.W., HETLING L.J., NOSAL M. & PAUSTIAN K. (2002) - *Sources of nitrate in rivers draining sixteen watersheds in the northeastern U.S.: Isotopic constrain.* Biogeochem., **57/58**, 171-197.

MINISSALE A., DONATO A., PROCESI M., PIZZINO L. & GIAMMANCO S. (2019) – *Systematic review of geochemical data from thermal springs, gas vents and fumaroles of Southern Italy for geothermal favourability mapping.* Earth-Sci Rev, **188**, 514-535.

MOOK W.G., BOMMERSON J.C. & STAVERMAN W.H. (1974) - *Carbon isotope fractionation between dissolved carbonate and gaseous carbon dioxide.* Earth Planet. Sci. Lett., **22**, 169-176.

NASELLI-FLORES L. (2008) - *Urban Lakes: Ecosystems at Risk, Worthy of the Best Care.* Proceedings of Taal: The 12th World Lake Conference: 1333-1337.

PARKHURST D.L. & APPELO C.A.J. (2013) - *Description of input and examples for PHREEQC version 3-A computer program for speciation, batch-reaction, one-dimensional transport, and inverse geochemical calculations.* U.S.G.S. Tech. Methods, book 6, chap. A43 497 available at: http://pubs.usgs.gov/tm/06/a43.

PEARCE C.R., PARKINSON I.J., GAILLARDET J., CHETELAT B. & BURTON K.W. (2015) - *Characterising the stable ($\delta^{88/86}Sr$) and radiogenic ($^{87}Sr/^{86}Sr$) isotopic composition of strontium in rainwater.* Chem. Geol., **409**, 54-60.

PIZZETTI I., SCHULZ F., TYML T., FUCHS B.M., AMANN R., HORN M. & FAZI S. (2016) - *Chlamydial seasonal dynamics and isolation of 'Candidatus Neptunochlamydia vexilliferae' from a Tyrrhenian coastal lake.* Environ. Microbiol., **18**, 2405-2417.

PIZZINO L., GALLI G., MANCINI C., QUATTROCCHI F. & SCARLATO P. (2002) - *Natural gas hazard (CO_2, ^{222}Rn) within a quiescent volcanic region and its relations with tectonics: the case of the Ciampino-Marino area, Alban Hills Volcano, Italy.* Nat. Hazards, **27**, 257-287.

PIZZINO L. (2015) - *"Fluid geochemistry and Natural Gas Hazard in the urban area of Rome"*. Tesi di dottorato, in italian, Università degli Studi Roma 3, 152 pp.

SALATA G.G., ROELKE L.A. & CIFUENTES L.A. (2000) - *A rapid and precise method for measuring stable isotope ratios of dissolved inorganic carbon.* Mar. Chem., **69**, 153-161.

SCHUELER T. & SIMPSON J. (2001) - *Why urban lakes are different.* Water Protection Techniques, **3**, 747-750.

SOBEK S., TRANVIK L.J., PRAIRIE Y.T., KORTELAINEN P. & COLE J. (2007) - *Patterns and regulation of dissolved organic carbon: An analysis of 7,500 widely distributed lakes.* Limnol. Oceanogr., **52**, 1208-1219.

TROMBETTA T., VIDUSSI F., MAS S., PARIN D., SIMIER M. & MOSTAJIR B. (2019) - *Water temperature drives phytoplankton blooms in coastal waters.* PloS ONE, **14**, e0214933.

TASSI F., FAZI S., ROSSETTI S., PRATESI P., CECCOTTI M., CABASSI J., CAPECCHIACCI F., VENTURI S. & VASELLI O. (2018) - *The biogeochemical vertical structure renders a meromictic volcanic lake a trap for geogenic CO_2 (Lake Averno, Italy).* PLoS ONE, **13**, e0193914.

TASSI F. & ROUWET D. (2014) - *An overview of the structure, hazards, and methods of investigation of Nyos-type lakes from the geochemical perspective.* J Limnol., **73**, 55-70.

TWARDOWSKI M.S., BOSS E., SULLIVAN J.M. & DONAGHAY P.L. (2004) - *Modeling the spectral shape of absorption by chromophoric dissolved organic matter.* Mar. Chem., **89**, 69-88.

VEIZER J. (1989) - *Strontium isotopes in seawater through time.* Ann. Rev. Earth Planet. Sci., **17**, 141-167.

WAGNER T. & ERICKSON L.E. (2017 - *Sustainable Management of Eutrophic Lakes and Reservoir.* J. Environ. Prot. Ecol., **8**, 436-463.

WASHINGTON H.S. (1906) The *Roman comagmatic region.* Carnegie Inst. Washington Publ., 57

WEISHAAR J.L., AIKEN G.R., BERGAMASCHI B.A., FRAM M.S., FUJI R. & MOPPER K. (2003) - *Evaluation of specific ultraviolet absorbance as an indicator of the chemical composition and reactivity of dissolved organic carbon.* Environ. Sci. Technol., **37**, 4702-4708.

WHITFIELD M. (1978) - *Activity coefficients in natural waters.* In: Pytkowicz, R.M. (Ed.), Activity Coefficients in Electrolyte Solutions. CRC Press, Boca Raton, FL, pp. 153-300.

ZHANG J, QUAY PD & WILBUR DO. (1995) - *Carbon isotope fractionation during gas-water exchange and dissolution of CO_2.* Geochim. Cosmochim. Acta, **59**, 107-114.